*Vijayalakshmi Ramalingam**

Department of Civil Engineering, Sri Sivasubramaniya Nadar College of Engineering, Chennai- 603110, India

Scientific paper
ISSN 0351-9465, E-ISSN 2466-2585
https://doi.org/10.62638/ZasMat1342

Zastita Materijala 67 ()
(2026)

Multi-scale behaviour of hybrid fiber reinforced recycled aggregate concrete: Mechanical and microstructural analysis

ABSTRACT

The use of recycled aggregate concrete (RAC) offers a sustainable solution for construction; however, its structural performance is often limited by weak interfacial transition zones (ITZ), increased porosity, and brittle failure behaviour. To address these limitations, the present study investigates the effectiveness of a multi-scale hybrid fiber reinforcement system incorporating steel fibers (SF) and polypropylene fibers (PP) in RAC. Concrete mixes with 25% and 50% recycled aggregate replacement were developed and reinforced with mono (SF0.5) and hybrid fiber combinations (SF0.75–PP0.25 and SF1–PP0.5). The mechanical behaviour was evaluated through compressive, splitting tensile, and flexural strength tests, along with detailed stress–strain analysis under uniaxial loading. The results demonstrated that hybrid fiber reinforcement significantly enhanced compressive strength (up to ~45 MPa), tensile capacity, and post-peak ductility compared to plain RAC. Digital image processing revealed a transition from localized cracking in control and RAC mixes to distributed microcracking in hybrid fiber systems, indicating improved crack control and stress redistribution. Microstructural analysis using scanning electron microscopy (SEM) confirmed the refinement of the ITZ and effective fiber–matrix interaction, where polypropylene fibers controlled microcrack initiation and steel fibers bridged macro cracks. Durability performance was assessed through water absorption and acid attack. While recycled aggregates increased permeability, hybrid fiber systems improved resistance to crack propagation and maintained structural integrity under aggressive conditions. However, excessive fiber content led to increased porosity, highlighting the need for optimal fiber dosage. Overall, the study demonstrates that the synergistic interaction between steel and polypropylene fibers can effectively mitigate the drawbacks of RAC and produce a durable, ductile, and high-performance sustainable concrete suitable for structural applications.

Keywords: *Recycled aggregate, steel fiber, polypropylene fiber, hybrid fiber, digital image processing. micro structural analysis, durability study.*

1. INTRODUCTION

The rapid growth of the construction industry has led to an increasing demand for natural aggregates, resulting in excessive depletion of natural resources and accumulation of construction and demolition (C&D) waste[2]. The reuse of recycled aggregates (RA) in concrete has emerged as a sustainable solution to address these challenges[3]. Recycled aggregate concrete (RAC) not only reduces environmental impact but also promotes circular economy practices in construction.

However, the incorporation of RA adversely affects the mechanical and durability properties of concrete due to the presence of adhered old mortar, higher porosity, and a weaker interfacial transition zone (ITZ) [4]. Previous studies have consistently reported reductions in compressive strength, stiffness, and durability performance with increasing RA content[5]. The inferior quality of RAC is primarily attributed to increased micro-cracking, higher water absorption, and reduced bond strength between aggregate and cement paste. These limitations restrict the widespread structural application of RAC, particularly in load-bearing and durability-critical structures [6]. Therefore, enhancing the performance of RAC through innovative material modification techniques remains a critical research area.

Fiber reinforcement has been widely adopted as an effective approach to improve the

Corresponding Author: Vijayalakshmi Ramalingam
Email: vijayalakshmir@ssn.edu.in
Paper received: 11.01.2026.
Paper corrected: 08.04. 2026.
Paper accepted: 23.04.2026.

mechanical and durability properties of concrete[7]. Fibers act as crack arresters, bridging cracks and redistributing stresses within the matrix[8]. Steel fibers (SF), owing to their high modulus of elasticity and tensile strength, are particularly effective in controlling macro cracks and improving post-peak behaviour, toughness, and energy absorption capacity of concrete[9]. On the other hand, polypropylene (PP) fibers, which are micro-scale fibrillated fibers, are highly effective in controlling plastic shrinkage cracks and microcrack initiation at early stages[10]. Recent advancements in fiber-reinforced concrete have focused on hybrid fiber systems, where two or more types of fibers are combined to achieve multi-scale crack control[11]. In such systems, micro fibers control the initiation and propagation of microcracks, while macro fibers bridge and arrest macro cracks, resulting in improved ductility and durability[12]. The synergistic interaction between fibers enhances the overall performance of concrete beyond that achievable with single fiber reinforcement[13].

Recent studies have extensively explored the application of hybrid fibers in RAC to overcome its inherent weaknesses. Gao et al. (2024) [14] investigated the cyclic compressive behaviour of hybrid fiber reinforced RAC and reported improved energy dissipation and reduced stiffness degradation. Similarly, Htet et al.(2024) [15] demonstrated enhanced deflection-hardening behaviour in hybrid fiber systems combining macro and micro fibers. Feng et al. (2023)[16] reported that steel–polypropylene hybrid fiber systems significantly improve the cyclic and post-peak behaviour of RAC by reducing crack width and enhancing load redistribution. Sun et al. (2025) [17] further highlighted that hybrid fibers improve the shear performance and durability characteristics of RAC through pore refinement and crack bridging mechanisms. Zhong et al. (2024)[18] observed that hybrid fibers enhance the microstructural properties of the ITZ, leading to improved bonding and reduced permeability.

In addition to mechanical performance, recent research has also emphasized durability aspects such as resistance to carbonation, acid attack, and water ingress. Studies by Liu et al. (2022)[19] and Wang et al. (2024) [20] indicate that hybrid fiber reinforcement reduces permeability and enhances resistance to aggressive environmental conditions by limiting crack connectivity and refining pore structure [21]. Digital image correlation and image processing techniques have also been increasingly used to quantify crack patterns and understand crack propagation mechanisms in fiber-reinforced concrete systems [22].

Despite significant advancements, most existing studies have primarily focused on combinations of steel fibers with other synthetic or mineral fibers such as basalt, glass, or PVA fibers[23]. Limited research has been conducted on the combined use of steel fibers and polypropylene fibers in recycled aggregate concrete, particularly in the context of multi-scale behaviour analysis [24].Furthermore, while several studies have investigated mechanical properties, there is a lack of comprehensive research integrating, Stress–strain behaviour, Failure pattern analysis, Digital image-based crack characterization, Microstructural (SEM) evaluation in a single unified framework. The absence of such integrated studies limits the understanding of the complete behaviour of hybrid fiber reinforced RAC.

The present study aims to address the identified research gaps by developing a multi-scale hybrid fiber reinforced recycled aggregate concrete (RAC) system incorporating steel fibers (SF) and polypropylene fibers (PP). Unlike previous studies, this work presents a comprehensive evaluation of both structural and durability performance through an integrated experimental and analytical approach. The novelty of this research lies in the use of a steel–polypropylene hybrid fiber system for effective multi-scale crack arresting, along with a detailed investigation of stress–strain behaviour and post-peak response under uniaxial compression. Furthermore, the study provides an in-depth analysis of failure patterns and ductility enhancement, supported by digital image processing techniques to quantify crack propagation and distribution. Microstructural characteristics are examined using SEM to understand ITZ behaviour and fiber–matrix interaction. Overall, the study demonstrates that the synergistic interaction between steel and polypropylene fibers can effectively compensate for the inherent deficiencies of recycled aggregates and enable the development of a durable, high-performance, and sustainable concrete suitable for structural applications.

2. EXPERIMENTAL INVESTIGATION

The experimental program was designed to evaluate the mechanical, durability, and microstructural performance of hybrid fiber reinforced recycled aggregate concrete (HFRRAC). A comprehensive testing methodology was adopted to investigate the influence of steel and polypropylene fibers on crack behaviour, strength characteristics, and long-term durability.Concrete specimens were cast for all nine mixes, including control, RAC 25, RAC 50, and their respective fiber-reinforced variants. The specimens were prepared under controlled laboratory conditions and cured in water at 27 ± 2°C until the testing age. The experimental program consisted of three major categories, mechanical behaviour, crack analysis and microstructure and durability performance.

2.1. Materials

The performance of hybrid fiber reinforced recycled aggregate concrete (HFRRAC) is governed by the characteristics of its constituent materials. In the present study, a carefully selected combination of cementitious materials, natural aggregates, recycled aggregates, and hybrid fibers was used to develop a multi-scale crack-resistant concrete system. The properties of materials used in the RAC concrete is discussed below. The image of the ingredients is shown in Fig.1. The particle size distribution of natural and recycled aggregate is shown in Fig. 2

Figure 1. Main ingredients for concrete mix (a) Cement (b) Gravel (c) Recycled Aggregate

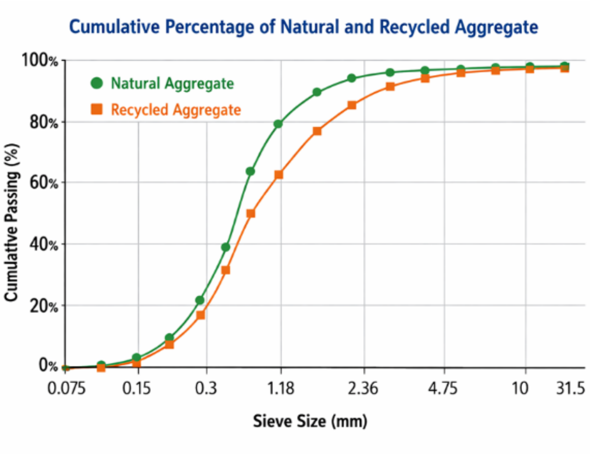

Figure 2. Cumulative percentage of Coarse Aggregate

(i) Cement

Ordinary Portland Cement (OPC) of 53 grade conforming to IS 12269 was used as the primary binder. The cement possessed a specific gravity of 3.15 and exhibited consistent quality suitable for structural-grade concrete. The choice of OPC was based on its ability to provide adequate early and long-term strength, ensuring compatibility with fiber reinforcement and recycled aggregates. The hydration process of cement plays a crucial role in forming calcium silicate hydrate (C–S–H) gel, which governs the strength and microstructural integrity of the concrete matrix.

(ii) Fine Aggregate

Locally available river sand conforming to Zone II grading as per IS 383 was used as fine aggregate. The sand had a specific gravity of 2.74 and was free from deleterious materials such as clay and organic impurities. The fine aggregate contributes to the packing density and workability of the concrete. A well-graded sand helps in minimizing voids and improving the bond between cement paste and aggregates, which is particularly important in RAC systems where the ITZ is inherently weaker.

(iii) Coarse Aggregate (Natural Aggregate)

Crushed limestone gravel with a nominal size of 10–20 mm was used as natural coarse aggregate. The aggregates were angular in shape and exhibited good mechanical strength. Natural aggregates provide the primary load-bearing skeleton in concrete and contribute to overall stiffness and strength.

(iv) Recycled Aggregate (RA)

Recycled coarse aggregates were obtained from crushed concrete debris and processed to achieve a size range of 18–20 mm. The recycled aggregates contained adhered mortar, resulting in higher porosity and water absorption compared to natural aggregates. These characteristics significantly influence the mechanical and durability performance of RAC.

Table 1. Physical Properties of Aggregates

Property	Natural Aggregate	Recycled Aggregate
Apparent Density (kg/m³)	2612	2410
Bulk Density (kg/m³)	1630	1470
Crushing Value (%)	15	19
Water Absorption (%)	1.76	4.89

The incorporation of RA introduces a weaker interfacial transition zone (ITZ) and increases internal microcracking. However, controlled replacement levels (25% and 50%) were adopted in this study to balance sustainability and performance. The physical properties of natural and recycled aggregates are presented in Table 1.

(v) Steel Fibers (Macro Fibers)

Hooked-end steel fibers were used as macro reinforcement in the concrete matrix. The steel fibers were selected due to their high tensile strength and modulus of elasticity, which enable effective bridging of macro cracks and enhancement of post-peak behaviour.The primary function of steel fibers in this study is to, arrest macro crack propagation, Improve load transfer across cracks, enhance ductility and energy absorption, delay failure under compressive loading

(vi) Polypropylene Fibers (Micro Fibers)

Fibrillated polypropylene (PP) fibers were used as micro reinforcement. These fibers possess low density and high flexibility, making them effective in controlling microcrack initiation at early stages of loading and during plastic shrinkage.The role of PP fibers includes, reduction of microcrack formation, control of plastic shrinkage cracks, improvement in pore structure , reduction in permeability and water ingress. The images of macro and micro fibers are shown in Fig. 3. The physical properties of the fibers are listed in Table 2.

Figure 3. (a) MacroSteel fiber and (b) Micro polypropylene fiber

Table 2. Properties of fibers

Property	Steel Fiber (SF)	Polypropylene Fiber (PP)
Type	Hooked-end	Fibrillated
Length (mm)	30–50	~20
Diameter (mm)	0.5–1.0	0.03
Aspect Ratio	50–80	High
Density (kg/m³)	7850	910
Tensile Strength (MPa)	1000–2000	350–500
Modulus of Elasticity (GPa)	~200	~3–5
Elongation (%)	2–5	25–30

2.2. Mix Design

The mix design for hybrid fiber reinforced recycled aggregate concrete (HFRRAC) was developed based on a target compressive strength of 40 MPa. A conventional design approach was adopted and subsequently modified to accommodate recycled aggregates and hybrid fiber incorporation. The primary objective was to achieve a balance between strength, workability, and durability while ensuring effective fiber dispersion.A constant water–cement ratio of 0.35 was maintained for all mixes to ensure comparable performance. The control mix was first designed using natural aggregates, and thereafter, natural coarse aggregates were partially replaced with recycled aggregates at 25% and 50% levels. These replacement levels were selected to represent moderate and high sustainability scenarios while maintaining structural applicability.

The introduction of recycled aggregates increases water demand due to their higher absorption capacity. To compensate for this effect, appropriate adjustments were made during mixing to maintain effective water content. However, the total water content was kept constant across all mixes to ensure uniform comparison of results. The mix proportion for each specimen ID is listed in Table 3.

Table 3. Mix proportion

Specimen ID	Cement (Kg/m^3)	*Gravel* (Kg/m^3)	*Recycled Aggregate* (Kg/m^3)	*Sand* (Kg/m^3)	Water (Kg/m^3)	Steel Fiber (Kg/m^3)	PP Fiber (Kg/m^3)
Control	450	650	1200	0	158	0	0
RAC 25	450	650	900	300	158	0	0
RAC 25-SF0.5	450	650	900	300	158	0.5	0
RAC 25-SF0.75-PP0.25	450	650	900	300	158	0.75	0.25
RAC 25-SF1-PP0.5	450	650	900	300	158	1.0	0.5
RAC 50	450	650	600	600	158	0	0
RAC 50-SF0.5	450	650	600	600	158	0.5	0
RAC 50-SF0.75-PP0.25	450	650	600	600	158	0.75	0.25

2.3. Fiber Dosage

The fiber dosage was selected based on the concept of multi-scale crack control, wherein macro and micro fibers act synergistically to enhance the performance of recycled aggregate concrete (RAC). Steel fibers (SF) were incorporated at three levels, namely 0.5% (low dosage, initiating macro crack control), 0.75% (intermediate level), and 1.0% (optimum level for structural performance), while polypropylene fibers (PP) were introduced at 0.25% (to initiate microcrack control) and 0.5% (to enhance microcrack arresting)[22]. The total fiber volume fraction was limited to 1.5% to avoid workability issues such as fiber clustering and balling [25]. The selected fiber combinations were systematically designed to investigate the individual contribution of steel fibers, evaluate the hybrid interaction between steel and polypropylene fibers, and identify the optimum combination for improving the mechanical and durability performance of RAC. The dosage of fibers is shown in Fig. 4

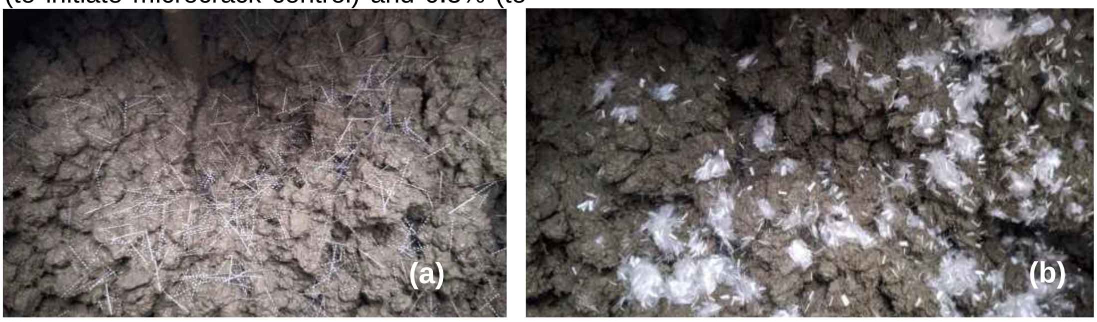

Figure 4. Addition of (a) Macro steel and (b) Micro polypropyleneFibers

2.4. Specimen Preparation

Fresh concrete was poured into the moulds in layers and compacted using a table vibrator to ensure proper consolidation and elimination of entrapped air. After casting, the specimens were covered to prevent moisture loss and demoulded after 24 hours. Subsequently, all specimens were cured in water until the designated age of testing. The specimens were prepared in accordance with the required test configurations, including cubes of size 150 × 150 × 150 mm for compressive strength, cylinders of 150 × 300 mm for splitting tensile strength, beams of 100 × 100 × 500 mm for flexural strength, and cubes of 100 × 100 × 100 mm for durability tests. Batching of materials, concrete prepration and demounding of cured specimen is shown in Fig. 5

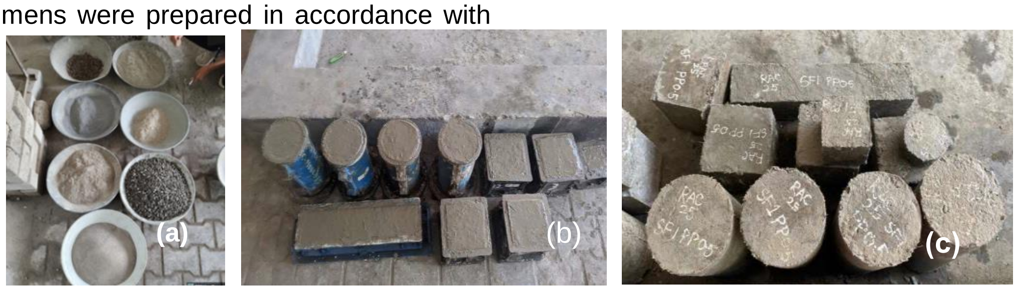

Figure 5. Specimen Prepration (a) Ingredients (b) Casting(c) Demoulding

2.5. Mechanical Testing

Compressive strength tests were conducted using a universal testing machine (UTM) with a loading rate of 0.5 MPa/s. Splitting tensile and flexural strength tests were performed as per relevant standards to evaluate tensile behaviour and crack resistance. Stress–strain behaviour was recorded using displacement-controlled loading to capture post-peak response. The mechanical testing setup is shown in Fig. 6. And the stress strain test setup in UTM for cylinder specimen is shown in Fig. 7.

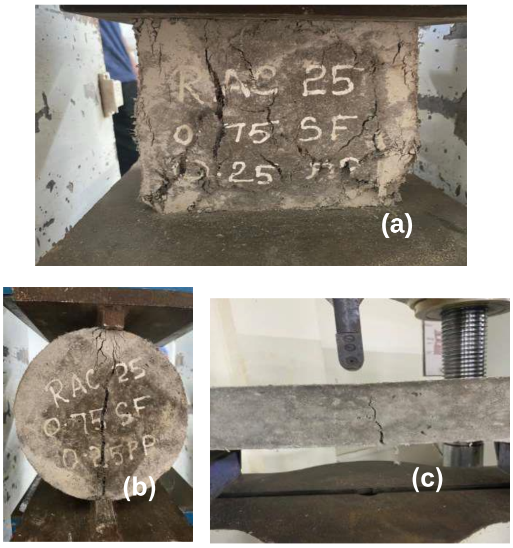

Figure 6. Compression, splitting and flexural strength test setup

Figure 7. Stress strain test setup for cylinders

2.6. Micro Structure analysis and Image Processing

Surface crack patterns were recorded using a high-resolution camera during loading. The images were processed using image analysis techniques to convert them into binary crack maps. Crack width, crack density, and crack propagation patterns were quantified to evaluate the effectiveness of fiber reinforcement in crack control.Scanning Electron Microscopy (SEM) was used to examine the microstructure of selected specimens. The focus was on analysing, Fiber–matrix bonding, Interfacial Transition Zone (ITZ), Crack bridging mechanisms, Hydration products. Samples were extracted from fractured specimens and prepared under vacuum conditions prior to SEM analysis.

3. RESULTS AND DISCUSSION

3.1. Failure patternof Recycled aggregate Concrete

3.1.1. Control, RAC 25 and RAC 50 (Plain Concrete Behaviour)

The control specimen exhibited a typical brittle failure mode under uniaxial compression, characterized by the formation of a dominant vertical crack initiating near the mid-height and propagating rapidly towards the loading faces. The failure occurred suddenly with minimal prior deformation, accompanied by surface spalling and crushing of concrete near the loading zone [6]. The crack pattern was highly localized, indicating poor stress redistribution capability. This behaviour is consistent with conventional concrete, where the absence of crack-arresting mechanisms leads to rapid crack coalescence and abrupt failure as shown in Fig 8(a).

In the case of RAC 25, the failure pattern showed a noticeable deviation from the control specimen. Although the failure remained predominantly brittle, the initiation of cracks occurred at lower stress levels due to the presence of weaker recycled aggregates and a porous interfacial transition zone (ITZ) [26]. Multiple microcracks were observed around the aggregate–paste interface, which gradually coalesced into a dominant crack as shown in Fig 8(b). The crack path was less uniform compared to the control, reflecting the heterogeneity introduced by recycled aggregates. The failure was still sudden; however, increased internal microcracking led to slightly reduced stiffness and earlier peak attainment.

For RAC 50, the failure behaviour became more pronouncedly brittle and unstable. The higher recycled aggregate content significantly weakened the matrix, resulting in early crack initiation and rapid crack propagation as shown in Fig 8 (c). Extensive surface spalling and fragmentation were observed, particularly near the loading faces. The crack pattern exhibited irregular propagation paths due to the non-uniform distribution of adhered mortar and weak ITZ zones. The specimen showed reduced load-carrying capacity and minimal post-peak deformation, confirming that increasing RA content adversely affects structural integrity and crack resistance [27].

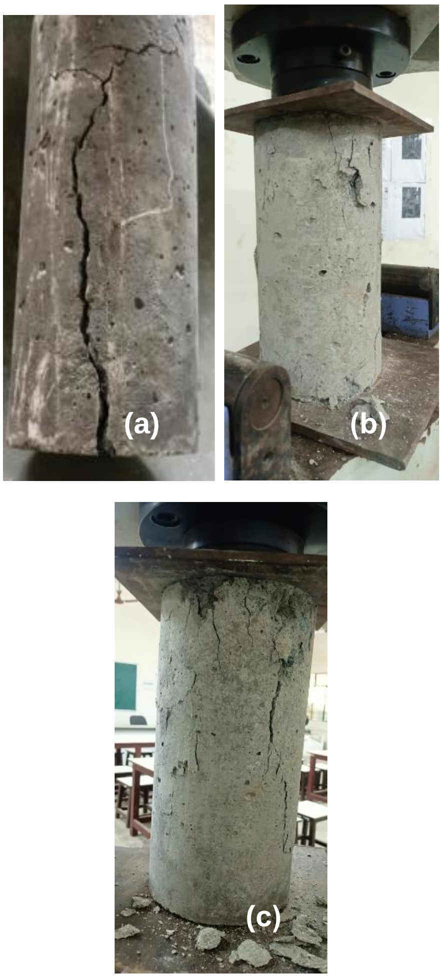

Figure 8. Uniaxial compression failure (a) Control concrete (b) RAC 25% (c) RAC 50%

3.1.2. RAC 25 and RAC 50 with Steel Fiber (SF0.5) – Single Fiber System

The incorporation of steel fibers (SF0.5) significantly altered the failure behaviour of RAC specimens by introducing a macro crack bridging mechanism. In RAC 25-SF0.5, the failure mode transitioned from brittle to semi-ductile behaviour. Crack initiation was delayed, and instead of a single dominant crack, multiple distributed cracks were observed across the specimen surface as shown in Fig.9 (a). Steel fibers effectively bridged the cracks, restricting their opening and preventing sudden propagation [28]. The failure occurred gradually, with reduced spalling and improved structural coherence.The crack pattern in RAC 25-SF0.5 was characterized by multiple fine cracks with limited width, indicating partial stress redistribution. However, crack localization was still evident in certain regions due to the absence of micro-level crack control [29]. The fibers were observed to resist crack widening rather than preventing crack initiation. As a result, the specimen exhibited moderate improvement in ductility and post-peak behaviour.

In RAC 50-SF0.5, the beneficial effect of steel fibers was evident but comparatively less pronounced. While the fibers improved crack bridging and reduced fragmentation, the inherent weakness of the RAC matrix limited the overall effectiveness. Crack initiation still occurred relatively early, but propagation was controlled to some extent by fiber action. The failure pattern showed reduced spalling compared to plain RAC 50, and the specimen retained its integrity even after peak load. However, localized cracking zones were still present, indicating that steel fibers alone are insufficient to fully compensate for the deficiencies of high recycled aggregate content [30]. The failure behaviour is shown in Fig.9(b).

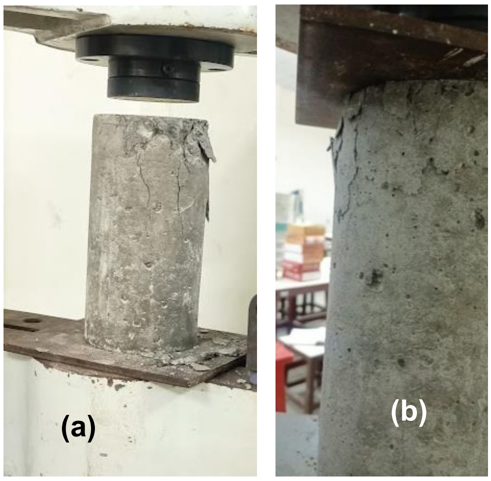

Figure 9. Uniaxial compression failure (a) RAC 25 with Steel fiber (b) RAC 50 with steel fiber

3.1.3. RAC 25 and RAC 50 with Hybrid Fiber Reinforcement (SF + PP)

The introduction of hybrid fibers (SF + PP) resulted in a significant transformation in failure behaviour, demonstrating a transition from brittle to highly ductile response. In RAC 25-SF0.75-PP0.25, crack initiation was substantially delayed due to the presence of polypropylene fibers, which effectively controlled microcrack formation at early stages. The steel fibers subsequently bridged the developing macro cracks, leading to a well-distributed crack network [31]. The failure pattern was characterized by multiple fine cracks with no dominant crack plane, indicating effective stress redistribution throughout the specimen.In the RAC 25-SF1-PP0.5 specimen, the failure mode exhibited pronounced ductility with minimal spalling and gradual post-peak softening[32]. The crack distribution was highly uniform, and the crack width was significantly reduced compared to both plain and mono-fiber specimens. The combined action of PP fibers and steel fibers resulted in a multi-scale crack arresting mechanism, where microcracks were suppressed at the initiation stage and macro cracks were prevented from widening[21]. This led to enhanced deformation capacity and improved energy absorption. The role of hybris fiber and the stress distribution of micro and macro fiber inside concrete is demonstrated in Fig. 10

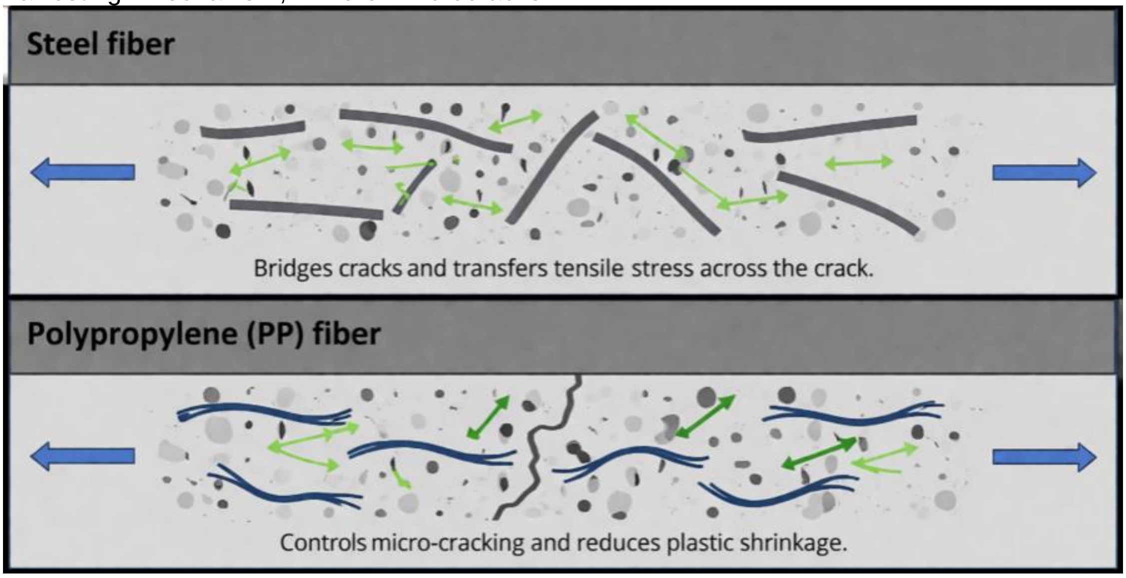

Figure 10. Stress distribution of macro fiber and fibrillated micro fibers

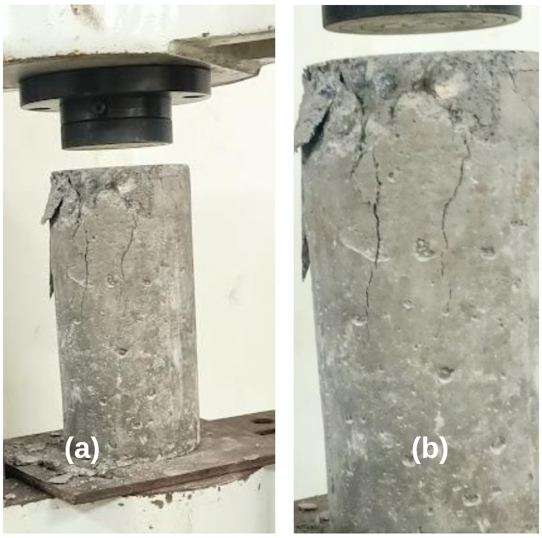

Figure 11. Uniaxial compression failure (a) RAC 25 with Steel +PP fiber (b) RAC 50 with hybrid fiber

For RAC 50 hybrid specimens, a similar trend was observed, although the overall performance remained slightly lower than RAC 25 due to higher inherent porosity. In RAC 50-SF0.75-PP0.25, the crack propagation was controlled effectively, with reduced crack width and improved cohesion compared to RAC 50-SF0.5. In RAC 50-SF1-PP0.5, the specimen exhibited the best performance among RAC 50 mixes, showing distributed cracking and minimal surface damage. The specimen retained its shape even after failure, indicating strong fiber bridging and enhanced matrix integrity[33].Overall, the hybrid fiber system demonstrated a synergistic interaction, where polypropylene fibers controlled micro-level damage and steel fibers resisted macro crack propagation [34]. This combination effectively eliminated crack localization, reduced spalling, and significantly improved ductility, confirming the superiority of hybrid fiber reinforcement in recycled aggregate concrete [35]. the failure pattern of hybrid fiber reinforced concrete is shown in Fig. 11

3.2. Stress Strain response of RAC

3.2.1. Control, RAC 25 and RAC 50 (Plain Concrete Behaviour)

The stress–strain response of the control specimen exhibited a typical brittle behaviour, characterized by a steep ascending branch followed by a sudden drop in the post-peak region. The peak stress was approximately 40.5 MPa, achieved at a strain of about 0.0022. Beyond the peak, the curve showed an abrupt decline, indicating negligible energy absorption and absence of crack-bridging mechanisms. This behaviour correlates well with the observed failure pattern, where rapid crack propagation led to collapse[21].For RAC 25, the peak stress reduced to approximately 39.2 MPa, with a slightly lower stiffness in the ascending branch. The reduction in stiffness and strength is attributed to the presence of recycled aggregates, which introduce microcracks and weaken the ITZ. The strain at peak stress showed a marginal increase (~0.0023), indicating slight deformability; however, the post-peak response remained brittle with rapid stress loss[36]. The curve shape suggests early microcrack initiation and reduced load transfer efficiency.

In RAC 50, the degradation in performance was more significant. The peak stress decreased further to approximately 38.0 MPa, and the ascending branch became less steep, indicating reduced elastic modulus. The peak strain increased (~0.0024), reflecting higher deformability due to increased porosity[37]. However, the post-peak region remained unstable, with sharp stress reduction. The overall behaviour confirms that higher recycled aggregate content leads to reduced strength, stiffness, and structural reliability[33]. The stress strain plot is shown in Fig. 12.

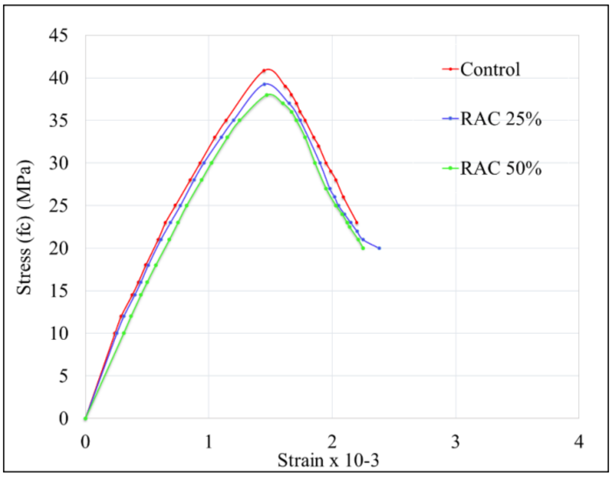

Figure 12. Stress strain response of control and RAC

3.2.2. RAC 25 and RAC 50 with Steel Fiber (SF0.5) – Single Fiber System

The incorporation of steel fibers significantly modified the stress–strain behaviour by enhancing post-peak ductility and load retention capacity. In RAC 25-SF0.5, the peak stress increased to approximately 41.5 MPa, which is notably higher than both plain RAC and equivalent plastic fiber systems reported earlier. This improvement is attributed to the higher modulus and tensile strength of steel fibers, which provide effective crack bridging and stress transfer[32].The ascending branch remained relatively similar to RAC 25; however, the peak region became broader, indicating improved strain tolerance. The peak strain increased to approximately 0.0026, reflecting enhanced deformation capacity. More importantly, the post-peak response showed a gradual reduction in stress, rather than a sudden drop[4]. This indicates that steel fibers effectively resisted crack widening and maintained load transfer even after peak stress.For RAC 50-SF0.5, the peak stress improved to approximately 40.2 MPa, showing recovery of strength despite higher RA content. The curve exhibited a less steep ascending branch compared to RAC 25, but the post-peak region showed significant improvement[38]. The stress decay was gradual, indicating improved toughness and energy absorption. However, the absence of micro-level crack control limited the overall performance, as microcracks continued to initiate early and coalesce under loading. The stress strain plot of RAC 25 and RAC 50 concrete with steel fibe reinforcement is shown in Fig. 13

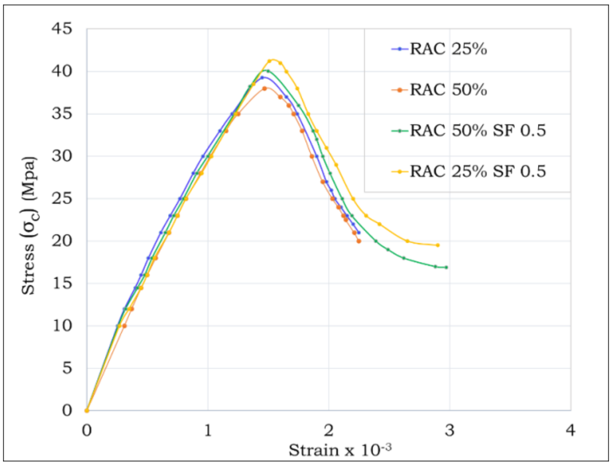

Figure 13. Stress Strain plot of RAC with steel fiber

3.2.3. RAC 25 and RAC 50 with Hybrid Fiber Reinforcement (SF + PP)

The hybrid fiber system produced the most significant enhancement in stress–strain behaviour, demonstrating a balanced improvement in strength, ductility, and post-peak performance. In RAC 25-SF0.75-PP0.25, the peak stress increased to approximately 43.5 MPa, representing a substantial improvement over both plain and mono-fiber mixes. The ascending branch showed improved stiffness due to better stress distribution, while the peak region became wider, indicating increased strain capacity (~0.0028).In the RAC 25-SF1-PP0.5 mix, the peak stress reached approximately 45.2 MPa, showing an increase of nearly 12–15% compared to RAC 25 and significantly higher than plastic fiber-based systems. The peak strain increased to approximately 0.0030, indicating enhanced deformability. The post-peak region exhibited a long tail with gradual stress reduction, reflecting high energy absorption and superior ductility. This behaviour confirms the synergistic interaction between steel and polypropylene fibers[39].For RAC 50 hybrid mixes, a similar trend was observed. In RAC 50-SF0.75-PP0.25, the peak stress increased to approximately 42.0 MPa, while RAC 50-SF1-PP0.5 reached 43.8 MPa, indicating significant strength recovery. The post-peak curves showed smooth descending branches with sustained load-carrying capacity, even at higher strains (~0.0031). The improved behaviour is attributed to the multi-scale crack arresting mechanism, where polypropylene fibers control microcrack initiation and steel fibers prevent macro crack propagationwhich is shown in Fig. 14

Overall, the hybrid fiber system effectively transformed the stress–strain response from brittle to ductile, with enhanced peak stress, increased strain capacity, and improved post-peak performance[40]. Compared to plastic fiber systems, steel fiber-based hybrids demonstrated superior stiffness, higher peak stress, and better load retention, confirming their suitability for structural applications involving recycled aggregate concrete. the stress strain response of RAC 25 and RAC 50 with hybrid fibe reinforcement is shown in Fig. 15 and Fig. 16 respectively.

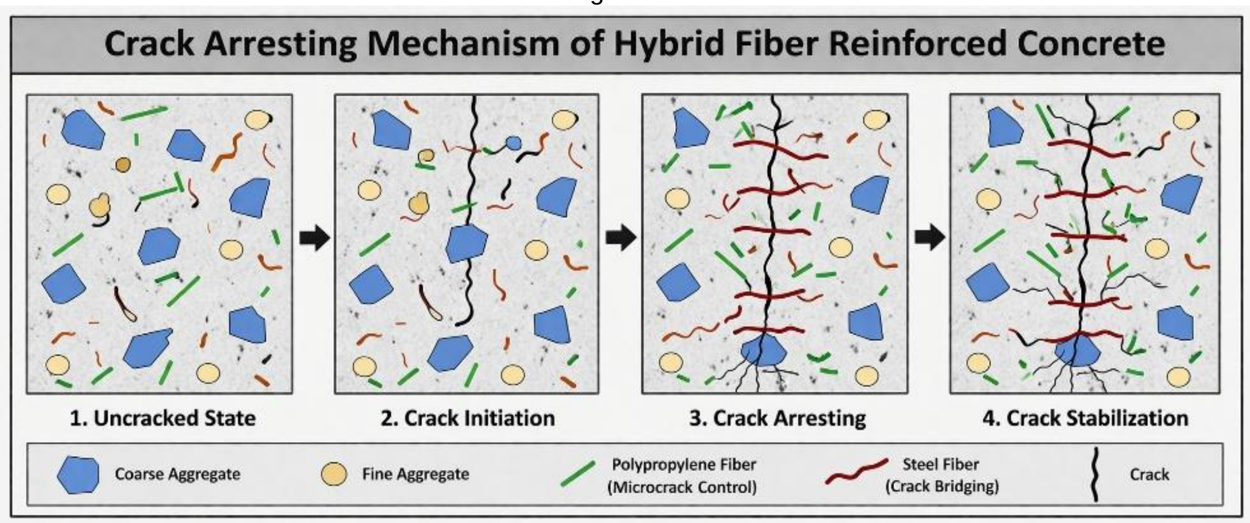

Figur 14. Crack Arresting mechanism of hybrid fiber reinforced concrete

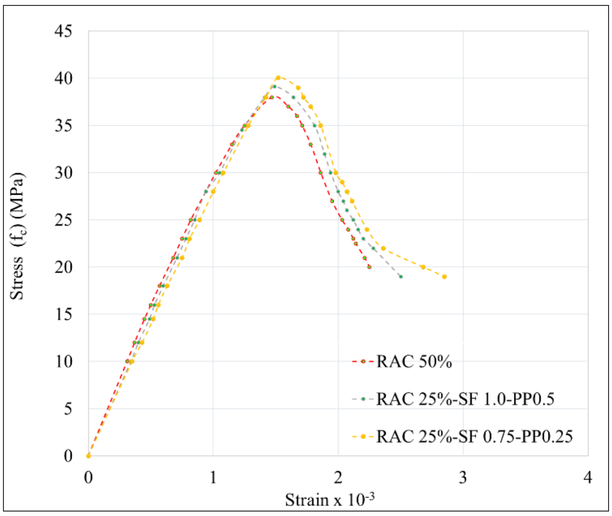

Figure 15. Stress Strain plot of RAC 25 with hybrid fiber

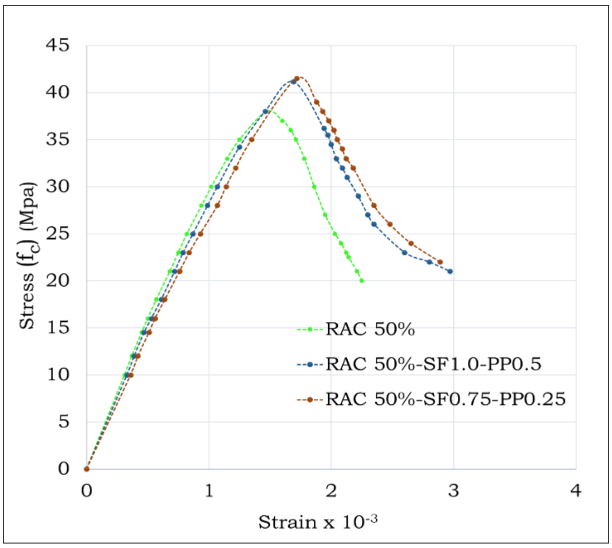

Figure 16. Stress Strain plot of RAC 50 with hybrid fiber

3.3. Mechanical strength of HFRRAC

3.3.1. Compressive Strength

The compressive strength results clearly demonstrate the influence of recycled aggregate content and fiber reinforcement on the load-carrying capacity of concrete. The control mix exhibited a peak compressive strength of 40.5 MPa, representing the baseline behaviour of a dense and well-bonded cementitious matrix. Upon replacing natural aggregates with recycled aggregates, a reduction in strength was observed. The RAC 25 mix showed a compressive strength of 39.2 MPa, while RAC 50 reduced further to 38.0 MPa, indicating a decrease of approximately 3.2% and 6.2%, respectively, compared to the control. This reduction is primarily attributed to the presence of adhered mortar, increased porosity, and weaker ITZ in recycled aggregates, which promote early crack initiation and reduce stress transfer efficiency.The incorporation of steel fibers improved the compressive strength of RAC mixes. The RAC 25-SF0.5 mix achieved 41.5 MPa, exceedingly even the control mix, while RAC 50-SF0.5 reached 40.2 MPa, indicating recovery of strength. The improvement is due to the ability of steel fibers to arrest macro cracks and provide confinement within the matrix. However, the increase remains moderate because compressive strength is largely governed by matrix properties rather than fiber action [41].

The hybrid fiber system exhibited the most significant improvement. The compressive strength increased to 43.5 MPa for RAC 25-SF0.75-PP0.25 and further to 45.0 MPa for RAC 25-SF1-PP0.5, representing an increase of nearly 14–15% compared to RAC 25. Similarly, RAC 50-SF1-PP0.5 achieved 43.8 MPa, indicating substantial recovery despite higher RA content [29]. This enhancement is attributed to the synergistic effect of fibers, where polypropylene fibers control microcrack initiation and steel fibers restrict macro crack propagation, leading to improved confinement and delayed failure. The results confirm that hybrid fiber reinforcement not only compensates for the loss in strength due to recycled aggregates but also enhances compressive performance beyond conventional concrete [26]. The failed cube specimen after compression test is shown in Fig 17(a-c).

Fig. 17 Cube Compression test of RAC and fiber reinforced RAC (a) Control (b) Single fiber RAC (c) Hybrid Fiber RAC

3.3.2. Splitting Tensile Strength

The splitting tensile strength results showed a more pronounced sensitivity to fiber reinforcement compared to compressive strength. The control mix exhibited a tensile strength of 2.75 MPa, which reduced to 2.62 MPa for RAC 25 and 2.48 MPa for RAC 50, indicating reductions of approximately 4.7% and 9.8%, respectively. The reduction is primarily due to the weak ITZ and increased microcracking associated with recycled aggregates, which significantly affect tensile behaviour since concrete is inherently weak in tension.The addition of steel fibers led to considerable improvement in tensile strength. The RAC 25-SF0.5 mix achieved 3.02 MPa, while RAC 50-SF0.5 reached 2.94 MPa, corresponding to increases of approximately 15–18% compared to their respective plain RAC mixes. Steel fibers effectively bridge cracks and transfer tensile stresses across the crack plane, delaying crack propagation and improving load-carrying capacity. The splitting tensile failure specimen is shown in Fig. 18(a-c).

The hybrid fiber mixes exhibited the highest tensile strength values. The RAC 25-SF0.75-PP0.25 mix reached 3.26 MPa, and the RAC 25-SF1-PP0.5 mix achieved 3.50 MPa, representing an increase of nearly 30–35% compared to RAC 25. Similarly, RAC 50-SF1-PP0.5 reached 3.40 MPa, showing a significant improvement of about 37% compared to RAC 50. This substantial enhancement is attributed to the combined action of micro and macro fibers[21]. Polypropylene fibers prevent the formation of microcracks at early stages, while steel fibers resist crack widening and ensure stress redistribution. As a result, crack initiation is delayed and crack propagation is controlled, leading to improved tensile resistance[42].

Figure 18. Splitting tensile strenght test specimen (a) RAC 25 (b) RAC 25-SF0.5 (c) RAC 50 SF-0.75-PPo.25

3.3.3. Flexural Strength

Flexural strength results followed a similar trend but with even greater sensitivity to fiber reinforcement due to the dominance of tensile stresses in bending. The control mix exhibited a flexural strength of 4.10 MPa, which reduced to 3.86 MPa for RAC 25 and 3.74 MPa for RAC 50, corresponding to reductions of approximately 5.8% and 8.8%, respectively. The reduction is associated with the weak tensile zone and poor crack resistance of RAC, which leads to early crack initiation under bending loads.The incorporation of steel fibers improved the flexural strength to 4.28 MPa for RAC 25-SF0.5 and 4.16 MPa for RAC 50-SF0.5, indicating improvements of about 10–11%. Steel fibers act as bridging elements across flexural cracks, increasing the load-carrying capacity and delaying crack propagation. However, their effectiveness is mainly observed after crack initiation [43]. The flexure test beam specimen is shown in Fig. 19.

The hybrid fiber system showed the highest flexural performance. The RAC 25-SF0.75-PP0.25 mix achieved 4.52 MPa, while the RAC 25-SF1-PP0.5 mix reached 4.72 MPa, representing an increase of approximately 20–22% compared to RAC 25. Similarly, RAC 50-SF1-PP0.5 achieved 4.56 MPa, indicating a substantial improvement over plain RAC 50. The enhanced flexural strength is attributed to the multi-scale crack control mechanism, where polypropylene fibers reduce crack initiation and steel fibers limit crack growth and widening[44]. This results in improved stress redistribution across the tensile zone and higher resistance to bending failure. The compression splitting and flexural strength of recycled aggregate concrete is shown in Fig. 20, Fig. 21 and Fig. 22 respectively. Overall, flexural strength showed the highest improvement among all mechanical properties, highlighting the effectiveness of hybrid fibers in resisting tensile stresses and controlling crack propagation under bending conditions. The peak stress, strain, and the maximum compressive , split and flexural strength are listed in Table 4

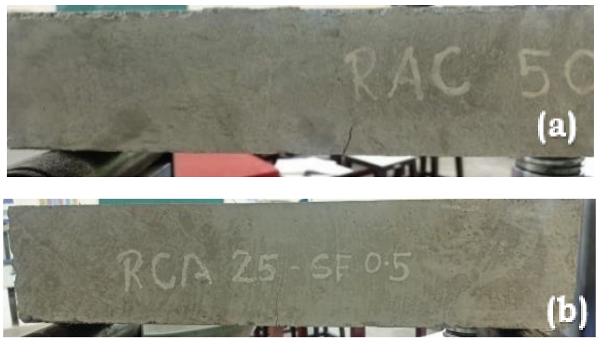

Figure19. Beam flexure test specimen (a) RAC 50 (b) RAC 25-SF 0.5

Table 4. Stress Strain values of recycled aggregate concrete

Specimen ID	f_{cu} N/mm^2	COV%	f_{st} N/mm^2	COV%	f_r N/mm^2	COV%
Control	34.0	2.52	2.75	1.52	4.10	1.12
RAC 25	32.5	2.81	2.62	2.12	3.86	2.21
RAC 25-SF0.5	36.5	3.01	3.02	1.25	4.28	2.34
RAC 25-SF0.75-PP0.25	39.0	2.71	3.26	2.24	4.52	1.23
RAC 25-SF1-PP0.5	41.5	3.00	3.50	1.21	4.72	2.34
RAC 50	30.8	3.37	2.48	1.56	3.74	1.24
RAC 50-SF0.5	34.8	3.03	2.94	2.32	4.16	1.12
RAC 50-SF0.75-PP0.25	37.5	3.09	3.18	2.05	4.38	2.13
RAC 50-SF1-PP0.5	39.8	3.20	3.40	1.28	4.56	1.24

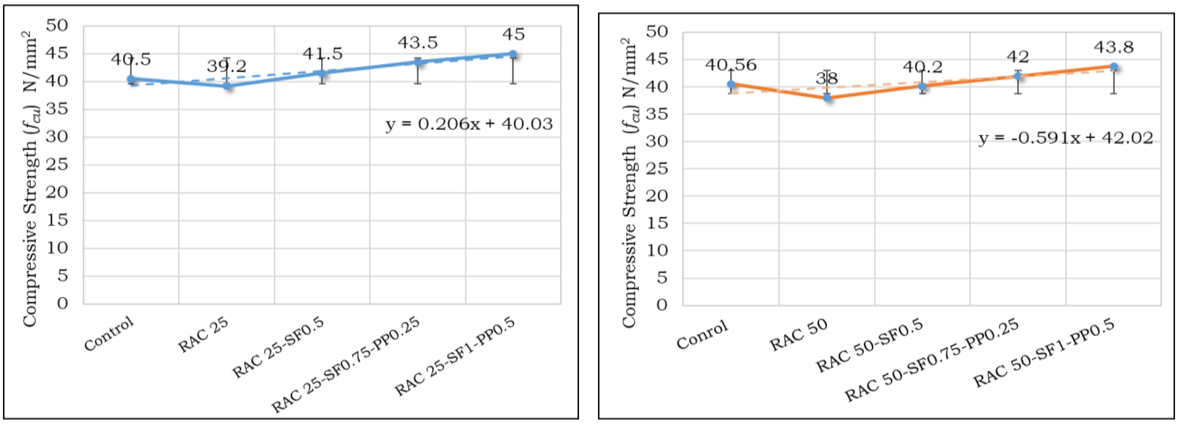

Figure 20. Cube Compressive Strength of hybrid fiber reinforced RAC

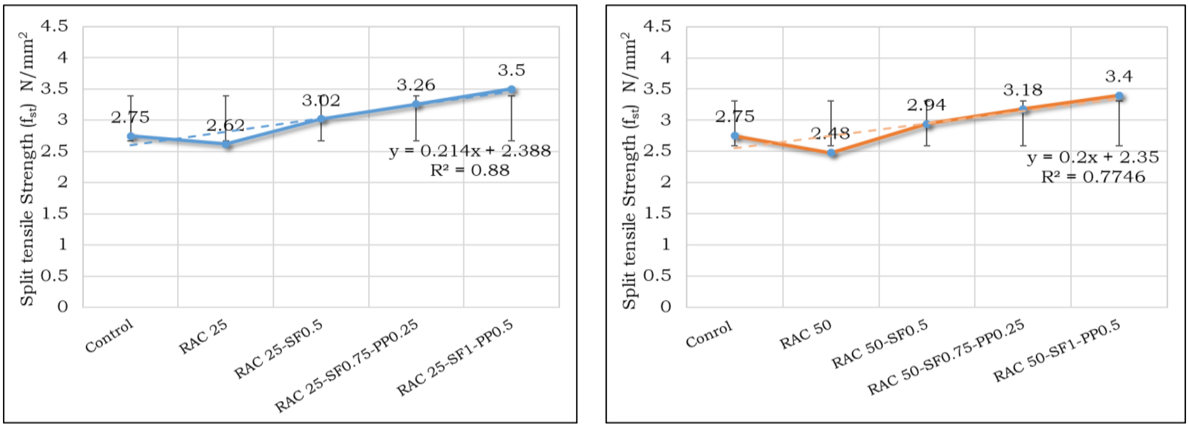

Figure 21. Splitting Tensile Strength of hybrid fiber reinforced RAC

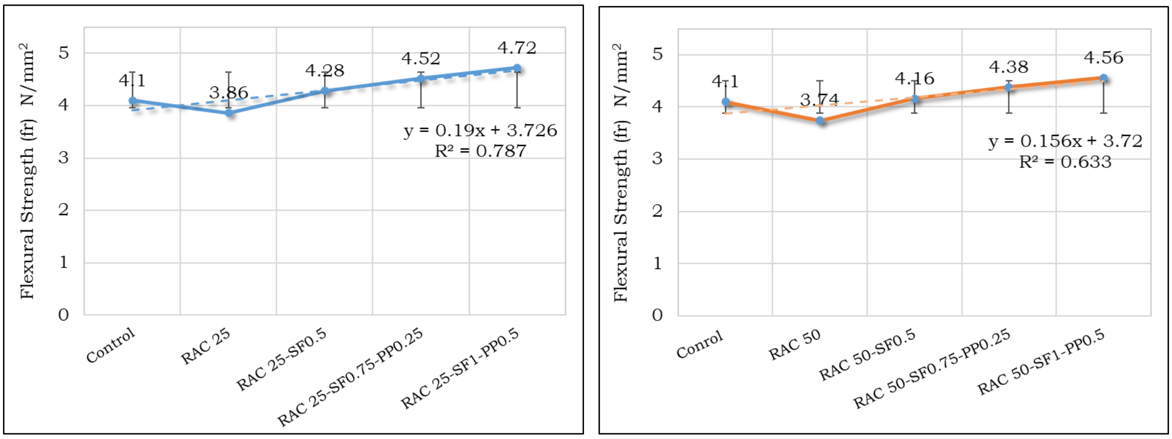

Figure 22. Flexural Strength of hybrid fiber reinforced RAC

3.4. Image processing of RAC concrete

3.4.1. Control, RAC 25 and RAC 50 (Plain Concrete Behaviour)

Digital image analysis of the control specimen revealed a highly localized crack pattern, characterized by the formation of a single dominant vertical crack extending from the mid-height toward the loading plates. The processed binary images showed low crack density but high crack width, indicating that once crack initiation occurred, the crack propagated rapidly without any resistance Fig 23(a). The absence of crack-bridging mechanisms resulted in poor stress redistribution, which is consistent with the abrupt post-peak drop observed in the stress–strain response. The crack width was significantly larger compared to fiber-reinforced specimens, confirming the brittle nature of conventional concrete.In the case of RAC 25, the crack pattern became more irregular and distributed compared to the control mix. The image analysis showed an increase in microcrack density, particularly around the aggregate–paste interface. These microcracks originated from the weaker ITZ associated with recycled aggregates and gradually coalesced into a dominant crack. Although the number of cracks increased, their distribution remained partially localized, and crack widths were still relatively high. This indicates that RAC introduces more internal damage zones but does not effectively prevent crack propagation[45].

For RAC 50, the crack pattern was highly heterogeneous, with multiple crack initiation points observed across the specimen surface. The binary images showed higher crack density than RAC 25, but with irregular crack paths and wider crack openings. The cracks propagated along weak zones formed by adhered mortar and porous aggregate surfaces[46]. The lack of any crack-arresting mechanism resulted in rapid crack coalescence and failure. The overall crack pattern confirms that increasing recycled aggregate content leads to higher internal damage, increased crack connectivity, and reduced resistance to crack propagation.

3.4.2. RAC 25 and RAC 50 with Steel Fiber (SF0.5)

The introduction of steel fibers significantly altered the crack pattern by reducing crack width and improving crack distribution. In RAC 25-SF0.5, the digital images showed a transition from a single dominant crack to multiple distributed cracks with reduced width as shown in Fig 23(b). The crack density increased compared to plain RAC, but the cracks were finer and less severe. This behaviour is attributed to the crack-bridging action of steel fibers, which resist crack opening and delay crack propagation. The fibers effectively transfer stresses across crack surfaces, preventing sudden crack widening.However, the image analysis also indicated that crack initiation was not significantly delayed. Microcracks still formed at early stages due to the inherent weakness of RAC[47]. The role of steel fibers was primarily observed in the post-cracking stage, where they controlled crack widening rather than preventing crack formation. As a result, although the crack width was reduced, some degree of crack localization was still present.In RAC 50-SF0.5, a similar trend was observed, but with slightly less effectiveness. The crack density increased, and crack widths were reduced compared to plain RAC 50, but the distribution remained uneven due to the highly porous matrix. Steel fibers were able to bridge macro cracks and prevent sudden failure, but they could not fully control the initiation of microcracks. The images confirmed that while steel fibers improve crack resistance, their effectiveness is limited when used alone, particularly in high recycled aggregate systems.

3.4.3. RAC 25 and RAC 50 with Hybrid Fiber Reinforcement (SF + PP)

The hybrid fiber system produced a significant transformation in crack behaviour, as clearly observed from the digital image analysis. In RAC 25-SF0.75-PP0.25, the crack pattern exhibited a high density of fine, uniformly distributed cracks with minimal crack width. The binary images showed a well-dispersed crack network, indicating effective stress redistribution throughout the specimen as shown in Fig. 23(c).

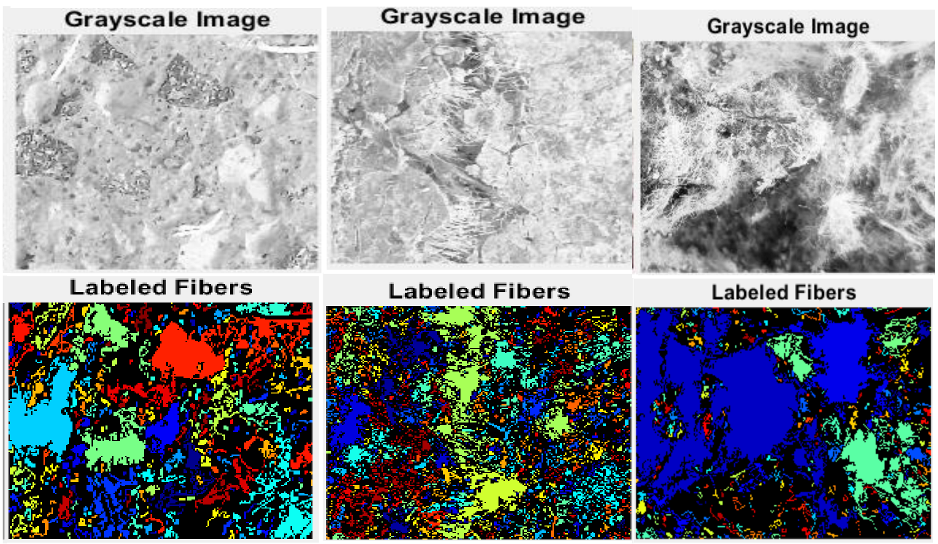

(a)RAC with Steel fiber (b) RAC 25-SF0.75-pp0.25 (c) RAC 50-SF1-PP0.5

Figure 23. Digital image of RAC with single and Hybrid fibre reinforcement

The polypropylene fibers played a crucial role in suppressing microcrack initiation, while steel fibers prevented the growth of larger cracks. This resulted in the elimination of crack localization and improved structural integrity.The most refined crack pattern was observed in RAC 25-SF1-PP0.5, where the cracks were extremely fine and evenly distributed across the surface. The crack width was significantly reduced compared to both plain and mono-fiber specimens, while the crack density was higher, indicating distributed cracking rather than localized failure. This behaviour is characteristic of a ductile material response, where energy is dissipated through multiple microcracks instead of a single dominant crack. The digital images clearly demonstrate the effectiveness of multi-scale crack control [48].

For RAC 50 hybrid mixes, the improvement was equally significant. In RAC 50-SF0.75-PP0.25, crack distribution became more uniform, and crack widths were reduced compared to RAC 50-SF0.5. In RAC 50-SF1-PP0.5, the crack pattern showed distributed microcracking with minimal crack coalescence, indicating strong fiber–matrix interaction. Despite the higher porosity of RAC 50, the hybrid fibers effectively reduced crack connectivity and prevented the formation of dominant cracks.Overall, the digital image analysis confirms that hybrid fiber reinforcement transforms the crack behaviour from localized brittle cracking to distributed ductile cracking. The increase in crack density combined with a significant reduction in crack width indicates enhanced stress redistribution, improved toughness, and superior durability performance. Compared to plastic fiber systems reported earlier, the steel–polypropylene hybrid system exhibited lower crack width, higher crack uniformity, and better crack control efficiency, making it more effective for structural applications.

3.5. Micro Structural analysis

3.5.1. Control, RAC 25 and RAC 50 (Matrix and ITZ Behaviour)

The microstructural analysis of the control specimen revealed a relatively dense and continuous cementitious matrix, dominated by well-developed C–S–H gel and limited pore connectivity. The interfacial transition zone (ITZ) between aggregate and paste appeared compact, with fewer microvoids and discontinuities. However, localized microcracks were still observed within the matrix, particularly near the ITZ, indicating stress concentration zones (Fig 24(a)). This microstructural configuration explains the relatively high compressive strength (40.5 MPa) of the control mix. Despite the dense matrix, the absence of any crack-arresting mechanism leads to rapid crack propagation once initiated, resulting in brittle post-peak behaviour and minimal ductility [21].

In RAC 25, the microstructure exhibited a more heterogeneous nature due to the presence of recycled aggregates. The ITZ around recycled aggregates was noticeably weaker, characterized by higher porosity, microcracks, and loosely packed hydration products. The adhered old mortar created a multi-layered ITZ, which reduced bonding efficiency and facilitated crack initiation. These microstructural defects directly correlate with the reduction in compressive strength (39.2 MPa) and tensile properties. The presence of interconnected pores and weak zones promotes early crack formation as shown in Fig 24(b), leading to reduced stiffness and unstable post-peak behaviour.

The microstructure of RAC 50 further amplified these deficiencies. A significantly higher number of microvoids, cracks, and weak ITZ regions were observed. The matrix appeared discontinuous, with poor bonding between aggregate and paste[49]. These features contribute to reduced load transfer efficiency and increased crack connectivity. As a result, the compressive strength dropped to 38.0 MPa, and the material exhibited highly brittle behaviour with rapid post-peak stress loss. The microstructure clearly indicates that increasing recycled aggregate content leads to a progressive deterioration of matrix integrity, which governs both strength reduction and lack of ductility.

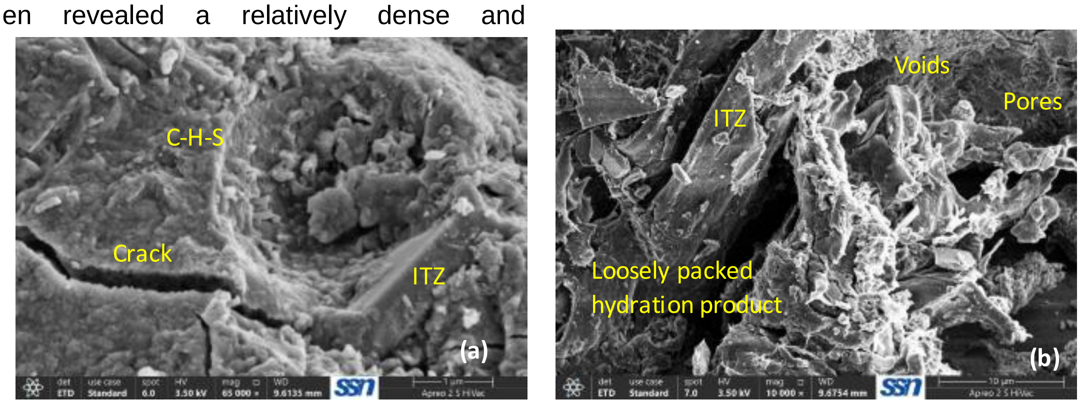

Figure 24. Micro Structural analysis of RAC 25 and RAC 50 concrete

3.5.2. RAC 25 and RAC 50 with Steel Fiber (SF0.5)

The introduction of steel fibers significantly modified the microstructural characteristics, particularly in terms of crack bridging and stress transfer mechanisms. SEM images of RAC 25-SF0.5 revealed that steel fibers were well embedded within the matrix, with hydration products forming around the fiber surface. This indicates strong mechanical anchorage and interfacial bonding, which is essential for effective crack bridging. Microcracks observed in plain RAC were now intercepted by steel fibers, preventing their propagation into macro cracks as shown in Fig 25. (a).

The improved microstructure explains the increase in compressive strength to 41.5 MPa and enhanced post-peak behaviour. Steel fibers act as load transfer bridges, redistributing stresses across cracked regions and delaying crack coalescence. This results in a more gradual stress reduction after peak load, indicating improved toughness. However, microcracks were still observed within the matrix, particularly in regions away from fibers, indicating that steel fibers primarily influence the macro-scale crack behaviour rather than microcrack initiation as shown in Fig. 25(b).

In RAC 50-SF0.5, the fibers were also observed to bridge cracks effectively, but the surrounding matrix remained relatively porous. The weak ITZ and high pore connectivity limited the effectiveness of fiber anchorage as shown in Fig. 25(c). Although compressive strength improved to 40.2 MPa, the enhancement was lower compared to RAC 25. The post-peak behaviour showed improvement, but the presence of microstructural defects led to localized failure zones. This indicates that while steel fibers improve ductility and energy absorption, their effectiveness is constrained by the quality of the surrounding matrix[50].

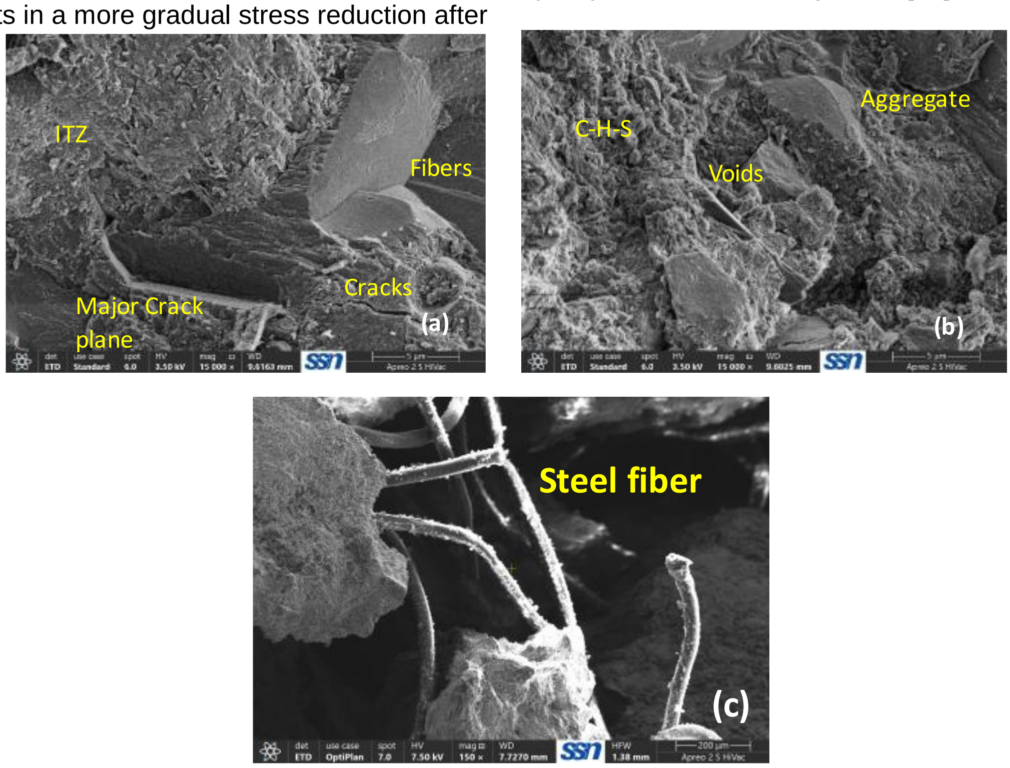

Figure 25. Microstructural image of Fiber reinforced Recycled aggregate concrete

3.5.3. RAC 25 and RAC 50 with Hybrid Fiber Reinforcement (SF + PP)

The hybrid fiber system produced the most refined and dense microstructure among all mixes. SEM images of RAC 25-SF0.75-PP0.25 showed a significant reduction in microcracks and pore connectivity. Polypropylene fibers were observed to be distributed within the matrix, forming a network that restricted microcrack initiation. These fibers do not rely on strong bonding but instead act as micro-scale crack arresters, preventing crack formation at early stages.Simultaneously, steel fibers were observed to bridge larger cracks, with hydration products tightly packed around the fiber surface, indicating strong interfacial bonding as shown in Fig. 26(a). This dual mechanism resulted in a highly stable microstructure with improved load transfer efficiency. The compressive strength increased to 43.5 MPa, and the post-peak behaviour showed a gradual decline, reflecting enhanced ductility and energy absorption. The combination of microcrack suppression and macro crack bridging led to a multi-scale reinforcement system, which significantly improved structural performance.

The most optimized microstructure was observed in RAC 25-SF1-PP0.5, where the matrix appeared highly compact with minimal microvoids. The ITZ was significantly improved, with reduced discontinuities and better bonding between aggregate and paste[5]. The polypropylene fibers effectively reduced microcrack density, while steel fibers prevented crack widening and propagation. This resulted in the highest compressive strength (45.0 MPa) and a pronounced ductile response with extended post-peak behaviour. The SEM images clearly indicate a synergistic interaction between fibers, leading to enhanced toughness and resistance to crack growth[51].

In RAC 50 hybrid mixes, similar improvements were observed despite the inherently weaker matrix. In RAC 50-SF1-PP0.5, the microstructure showed reduced pore connectivity and improved ITZ compared to plain RAC 50 as shown in Fig 26(b). The fibers compensated for the weaknesses of recycled aggregates by controlling crack formation and propagation. The compressive strength increased to 43.8 MPa, and the post-peak response exhibited a smoother decline, indicating improved ductility. The hybrid fibers effectively reduced crack connectivity as shown in Fig. 26 (c), which is critical for both strength and durability[6].

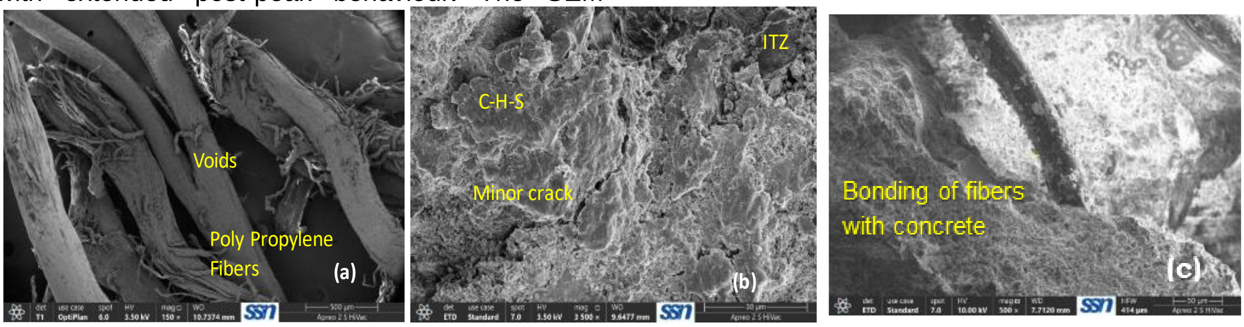

Figure 26. Micro Structural analysis of Hybris Fiber reinforced recycled aggregate concrete

4. CONCLUSION

- The incorporation of recycled aggregates resulted in a reduction in mechanical performance due to weaker interfacial transition zones (ITZ), increased porosity, and higher microcrack density, leading to relatively brittle behaviour compared to conventional concrete.
- The addition of steel fibers (SF) improved compressive, splitting tensile, and flexural strengths by effectively bridging macro cracks and enhancing post-peak load-carrying capacity, thereby improving overall structural response.
- Hybrid fiber reinforcement (SF+PP) demon-strated superior performance compared to mono-fiber systems, owing to the synergistic action of polypropylene fibers controlling microcrack initiation and steel fibers restricting macro crack propagation.
- The hybrid mixes with SF1–PP0.5 exhibited the highest mechanical performance, achieving enhanced compressive strength, tensile capacity, and flexural strength along with improved peak strain and ductility.
- Stress–strain behaviour showed a clear transition from brittle to ductile response with fiber inclusion, particularly in hybrid systems, which exhibited a gradual post-peak decline and higher energy absorption capacity.
- Digital image processing confirmed a shift from localized cracking in control and plain RAC mixes to uniformly distributed microcracking in fiber-reinforced specimens, indicating improved crack control and stress redistribution.
- Microstructural analysis (SEM) revealed that hybrid fiber systems led to a refined matrix, improved ITZ characteristics, reduced crack connectivity, and effective fiber–matrix interaction, which directly contributed to enhanced mechanical behaviour.
- The combined use of steel and polypropylene fibers effectively compensated for the inherent deficiencies of recycled aggregate concrete, resulting in improved strength, ductility, and structural integrity.
- Overall, hybrid fiber reinforced RAC can be considered a sustainable and high-performance material suitable for structural applications, offering a viable solution for the effective utilization of recycled aggregates.

Author statement

Vijayalakshmi Ramalingam: Investigation, Data Curation, Formal analysis, Writing -Original Draft.

Orchid ID : https://orcid.org/0000-0003-4678-2020

Declaration of competing interest

The authors declare that they have no known competing financial interests or personal relationships that could have appeared toinfluence the work reported in this paper.

Data availability

Data will be made available on request.

Acknowledgement

The author would like to acknowledge the support provided by the management of Sri Sivasubramaniya Nadar College of Engineering, Department of Civil Engineering, for facilitating this investigation at the Advanced Material Testing Laboratory. Additionally, the author extends gratitude to the Research Centre at Sri Sivasubramaniya Nadar College of Engineering, Department of EEE, for providing the microstructural FESEM image data.

5. REFERENCE

[1] L. Hong, W. Tang, Y. Tan, Y. Wang, Q. Yu (2025) Effect of short fibers on non-uniform strain distribution of geopolymer mortar under dry conditions, Constr. Build. Mater., 459, 139768, doi:10.1016/j.conbuildmat.2024.139768.

[2] L. Niu, X. Nie, N. Li, J. Guan, L. Li, C. Xie (2026) Experimental and theoretical investigation of fiber-reinforced geopolymer mortars: Mix design optimization and bond behavior with brick masonry, Case Stud. Constr. Mater., 24, e05767, doi:10.1016/j.cscm.2026.e05767.

[3] M. Nedeljković, N. Tošić, E. Schlangen, S. Fennis (2023) Pre-demolition concrete waste stream identification: Classification framework, Gradjevinski Mater. iKonstr., 66(1), 1–24, doi:10.5937/grmk2301001n.

[4] M. Dai, H. Ou, P. Kuang, Z. Lu, B. Yuan, J. Xie (2024) Study on the mechanical property and durability of alkali-activated seawater and sea sand recycled aggregate concrete, J. Build. Eng., 98, 111157, doi:10.1016/j.jobe.2024.111157.

[5] K. Zhang, W. Lin, Q. Lan, Q. Zhang (2024) Compressive properties of polypropylene fiber reinforced seawater sea-sand recycled aggregate concrete under different strain rate loading, Constr. Build. Mater., 452, 138968, doi:10.1016/j.conbuildmat.2024.138968.

[6] C. Wang, J. Yuan, Y. Zhang, Z. Ma (2024) Study on the mesoscopic mechanical behavior and damage constitutive model of micro-steel fiber reinforced recycled aggregate concrete, Constr. Build. Mater., 443, 137767, doi:10.1016/j.conbuildmat.2024.137767.

[7] M. GA, V. Mehdi, M. Javadi, A. Parvari (2024) Durability and compressive strength of composite polyolefin fiber-reinforced recycled aggregate concrete: An experimental study, Compos. Part C Open Access, 100533, doi:10.1016/j.jcomc.2024.100533.

[8] R. Sathia, R. Vijayalakshmi (2021) Fresh and mechanical property of caryota-urensfiber reinforced flowable concrete, J. Mater. Res. Technol., 15, 3647–3662, doi:10.1016/j.jmrt.2021.09.126.

[9] S. Abdallah, D.W.A. Rees, S.H. Ghaffar, M. Fan (2018) Understanding the effects of hooked-end steel fibre geometry on the uniaxial tensile behaviour of self-compacting concrete, Constr. Build. Mater., 178, 484–494, doi:10.1016/j.conbuildmat.2018.05.191.

[10] J. Branston, S. Das, S.Y. Kenno, C. Taylor (2016) Influence of basalt fibres on free and restrained plastic shrinkage, Cem. Concr. Compos., 74, 182–190, doi:10.1016/j.cemconcomp.2016.10.004.

[11] Y. Yang, Q. Zhou, Y. Deng, J. Lin (2022) Reinforcement effects of multi-scale hybrid fiber on flexural and fracture behaviors of ultra-low-weight foamed cement-based composites, Cem. Concr. Compos., 128, 104422, doi:10.1016/j.cemconcomp.2022.104422.

[12] F.K. Alqahtani, I. Zafar (2021) Plastic-based sustainable synthetic aggregate in green lightweight concrete – A review, Constr. Build. Mater., 292, 123321, doi:10.1016/j.conbuildmat.2021.123321.

[13] O.Y. Bayraktar, S.S.T. Eshtewı, A. Benli, G. Kaplan, K. Toklu, F. Gunek (2021) The impact of RCA and fly ash on the mechanical and durability properties of polypropylene fibre-reinforced concrete exposed to freeze-thaw cycles and $MgSO_4$ with ANN modeling, Constr. Build. Mater., 313, 125508, doi:10.1016/j.conbuildmat.2021.125508.

[14] H. Gao, et al. (2024) Cyclic compressive behavior of high-performance hybrid fiber reinforced recycled aggregate concrete: Degradation law and acoustic emission features, Constr. Build. Mater., 431, 136412, doi:10.1016/j.conbuildmat.2024.136412.

[15] P. Htet, W. Chen, Z. Huang, H. Hao (2024) Physical and mechanical properties of deflection-hardening hybrid fibre-reinforced recycled aggregate concrete, J. Build. Eng., 90, 109510, doi:10.1016/j.jobe.2024.109510.

[16] J. Feng, X. Jia, X. Dong, P. Wang, B. Xu, Z. Wang (2023) Cyclic compressive behavior of hook-end steel and macro-polypropylene hybrid fiber reinforced recycled aggregate concrete, Case Stud. Constr. Mater., 19, e02310, doi:10.1016/j.cscm.2023.e02310.

[17] M. Sun, et al. (2025) Mechanical and micro-structural properties of graphite tailings based geopolymer mortars at high temperature, Case Stud. Constr. Mater., 23, e05388, doi:10.1016/j.cscm.2025.e05388.

[18] C. Zhong, et al. (2025) Experimental investigation on flexural fatigue performance of recycled aggregate concrete hybrid with basalt-polyacrylonitrile fiber, Sci. Rep., 15, 5855, doi:10.1038/s41598-025-89682-x.

[19] H. Liu, Q. Li, S. Ni (2022) Assessment of the engineering properties of biomass recycled aggregate concrete developed from coconut shells, Constr. Build. Mater., 342, 128015, doi:10.1016/j.conbuildmat.2022.128015.

[20] C. Wang, J. Liu, B. Lu, Y. Zhang, Z. Ma (2024) Stiffness degradation and mechanical behavior of microfiber-modified high-toughness recycled aggregate concrete under constant load cycling, Eng. Fract. Mech., 312, 110608, doi:10.1016/j.engfracmech.2024.110608.

[21] K. Cui, et al. (2023) Mechanical behavior of multiscale hybrid fiber reinforced recycled aggregate concrete subject to uniaxial compression, J. Build. Eng., 71, 106504, doi:10.1016/j.jobe.2023.106504.

[22] A. Vahidi, A. Mostaani, A.T. Gebremariam, F. Di Maio, P. Rem (2024) Feasibility of utilizing recycled coarse aggregates in commercial concrete production, J. Clean. Prod., 474, 143578, doi:10.1016/j.jclepro.2024.143578.

[23] M. Ziada, H. Tanyildizi, A. Coskun (2025) Mechanical and microstructural properties of basalt fiber reinforced underwater geopolymer mortar, Structures, 75, 108814, doi:10.1016/j.istruc.2025.108814.

[24] A.A. Elakhras, M.H. Seleem, H.E.M. Sallam (2021) Intrinsic fracture toughness of fiber reinforced and functionally graded concretes: An innovative approach, Eng. Fract. Mech., 258, 108098, doi:10.1016/j.engfracmech.2021.108098.

[25] M. Ozawa, H. Morimoto (2014) Effects of various fibres on high-temperature spalling in high-performance concrete, Constr. Build. Mater., 71, 83–92, doi:10.1016/j.conbuildmat.2014.07.068.

[26] Y. Yu, L. Zhou, Z. Liao, Y. Zheng (2024) Tension stiffening and cracking behaviors in glass fiber reinforced polymer bar enhanced precast recycled aggregate concrete specimen, *Structures*, 69, 107395, doi:10.1016/j.istruc.2024.107395.

[27] P. Zhu, X. Chen, H. Liu, Z. Wang, C. Chen, H. Li (2024) Recycling of waste recycled aggregate concrete in freeze-thaw environment and emergy analysis of concrete recycling system, *J. Build. Eng.*, 96, 110377, doi:10.1016/j.jobe.2024.110377.

[28] [S. Tejas, D. Pasla (2024) Approach to design sustainable alkali-activated slag recycled aggregate concrete: Mechanical and microstructural characterization, *Case Stud. Constr. Mater.*, 21, e03886, doi:10.1016/j.cscm.2024.e03886.

[29] H. Wu, J. Zhang, Y. Chen, R. Jiang, Z. Zhu, P. Li (2024) Stress-strain behavior and failure criterion study of polypropylene fiber reinforced recycled aggregate concrete under triaxial stress state, *Constr. Build. Mater.*, 448, 138185, doi:10.1016/j.conbuildmat.2024.138185.

[30] [S. Haruehansapong, P. Khamput, P. Yoddumrong (2024) Enhancement of recycled aggregate concrete properties through the incorporation of nanosilica and natural fibers, *Heliyon*, 10, e39924, doi:10.1016/j.heliyon.2024.e39924.

[31] W. Xu, et al. (2024) Mechanical properties and constitutive relation of recycled aggregate concrete reinforced with face mask fibre and basalt fibre under uniaxial cyclic compression, *Structures*, 69, 107364, doi:10.1016/j.istruc.2024.107364.

[32] C. Wang, J. Yuan, Y. Zhang, Z. Ma (2024) A comparative study of low cyclic loading effects on plastic strain, nonlinear damping, and strength softening in fiber-reinforced recycled aggregate concrete, *J. Build. Eng.*, 97, 110774, doi:10.1016/j.jobe.2024.110774.

[33] J. Pereiro-Barceló, E. Lenz, B. Torres, L. Estevan (2024) Mechanical properties of recycled aggregate concrete reinforced with conventional and recycled steel fibers and exposed to high temperatures, *Constr. Build. Mater.*, 452, 138976, doi:10.1016/j.conbuildmat.2024.138976.

[34] X. Meng, Y. Chi, Q. Jiang, R. Liu, K. Wu, S. Li (2019) Experimental investigation on the flexural behavior of pervious concrete beams reinforced with geogrids, *Constr. Build. Mater.*, 215, 275–284, doi:10.1016/j.conbuildmat.2019.04.217.

[35] M.A. Al-Osta, A.S. Al-Tamimi, S.M. Al-Tarbi, O.S.B. Al-Amoudi, W.A. Al-Awsh, T.A. Saleh (2022) Development of sustainable concrete using recycled high-density polyethylene and crumb tires: Mechanical and thermal properties, *J. Build. Eng.*, 45, 103399, doi:10.1016/j.jobe.2021.103399.

[36] L. Dadd, B. Bennett, T. Xie, P. Visintin (2025) Shear behaviour and environmental impact of single and multi-generation recycled aggregate concrete beams, *Eng. Struct.*, 322, 119200, doi:10.1016/j.engstruct.2024.119200.

[37] M.L. Kasulanati, R.K. Pancharathi (2024) Optimizing multi-recycled concrete for sustainability: Aggregate gradation, surface treatment methods and life cycle impact assessment, *Constr. Build. Mater.*, 449, 138510, doi:10.1016/j.conbuildmat.2024.138510.

[38] J. Dong, Y. Ding, Y. Liu, Z. Ning, Y. Qi (2024) Tensile test and discrete element study on recycled aggregate hydraulic asphalt concrete, *Constr. Build. Mater.*, 450, 138538, doi:10.1016/j.conbuildmat.2024.138538.

[39] B. Kanagaraj, S. Shaji, M. Jafrin, S. Raj R, N. Anand, E. Lubloy (2024) Natural and synthetic fiber reinforced recycled aggregate concrete subjected to standard fire temperature, *Heliyon*, 10, e39676, doi:10.1016/j.heliyon.2024.e39676.

[40] R. Vijayalakshmi, A.G. Sriram, R. Prakash, N. Divyah, R. Geetha (2025) Micro structure analysis and digital image processing of monofilament and fibrillated fiber reinforced recycled aggregate concrete, *Struct. Eng. Mech.*, 1, 65–89.

[41] H. Gao, et al. (2024) Cyclic compressive behavior of high-performance hybrid fiber reinforced recycled aggregate concrete: Degradation law and acoustic emission features, *Constr. Build. Mater.*, 431, 136412, doi:10.1016/j.conbuildmat.2024.136412.

[42] X. Cong, et al. (2022) Study on the effectiveness of fibre reinforcement on the engineering performance of foamed concrete, *Case Stud. Constr. Mater.*, 16, e01015, doi:10.1016/j.cscm.2022.e01015.

[43] Y. Ji, Q. Sun (2023) Experimental and numerical investigation of recycled rubber foam concrete, *Alexandria Eng. J.*, 76, 573–594, doi:10.1016/j.aej.2023.06.057.

[44] X. Zhang, J. Wang, C. Lou (2024) Experimental study on axial tensile properties of basalt fibre reinforced recycled aggregate concrete, *Heliyon*, 10, e34208, doi:10.1016/j.heliyon.2024.e34208.

[45] H. Zhou, H. Li, A. Abdelhady, X. Liang, H. Wang, B. Yang (2019) Experimental investigation on the effect of pore characteristics on clogging risk of pervious concrete based on CT scanning, *Constr. Build. Mater.*, 212, 130–139, doi:10.1016/j.conbuildmat.2019.03.310.

[46] J. Justs, M. Wyrzykowski, D. Bajare, P. Lura (2015) Internal curing by superabsorbent polymers in ultra-high performance concrete, *Cem. Concr. Res.*, 76, 82–90, doi:10.1016/j.cemconres.2015.05.005.

[47] Y. Lu, L. Duanmu, Z. Zhai, Z. Wang (2022) Application and improvement of Canny edge-detection algorithm for exterior wall hollowing detection using infrared thermal images, *Energy Build.*, 274, 112421, doi:10.1016/j.enbuild.2022.112421.

[48] X. Li, H. Lin, W. Chen, S. Liang, L. Huang (2023) A numerical study on the tensile splitting of concrete with digital image processing, *J. Mater. Res. Technol.*, 25, 1626–1641, doi:10.1016/j.jmrt.2023.06.026.

[49] N.U. Kockal, T. Ozturan (2011) Durability of lightweight concretes with lightweight fly ash aggregates, *Constr. Build. Mater.*, 25(3), 1430–1438, doi:10.1016/j.conbuildmat.2010.09.022.

[50] R. Vijayalakshmi, M. Vaishnavi, R. Geetha (2023) Study on the workability and mechanical properties of fish tail palm fibre reinforced concrete: Emphasis on fibre content and fibre length, *Eur. J. Environ. Civ. Eng.*, 27(4), 1484–1502.

[51] A. Toghroli, P. Mehrabi, M. Shariati, N.T. Trung, S. Jahandari, H. Rasekh (2020) Evaluating the use of recycled concrete aggregate and pozzolanic additives in fiber-reinforced pervious concrete with industrial and recycled fibers, *Constr. Build. Mater.*, 252, 118997, doi:10.1016/j.conbuildmat.2020.118997.

IZVOD

VIŠERAZMERNO PONAŠANJE HIBRIDNOG RECIKLIRANOG AGREGATNOG BETONA ARMIRANOG VLAKNIMA: MEHANIČKA I MIKROSTRUKTURNA ANALIZA

Upotreba recikliranog agregatnog betona (RAC) nudi održivo rešenje za građevinarstvo; međutim, njegove strukturne performanse su često ograničene slabim međupovršinskim prelaznim zonama (ITZ), povećanom poroznošću i krhkim ponašanjem pri lomu. Da bi se rešila ova ograničenja, ova studija istražuje efikasnost višerazmernog hibridnog sistema armiranja vlaknima koji uključuje čelična vlakna (SF) i polipropilenska vlakna (PP) u RAC-u. Betonske mešavine sa 25% i 50% zamene recikliranog agregata su razvijene i armirane mono (SF0.5) i hibridnim kombinacijama vlakana (SF0.75–PP0.25 i SF1–PP0.5). Mehaničko ponašanje je procenjeno testovima čvrstoće na pritisak, zateznu čvrstoću cepanje i savijanje, zajedno sa detaljnom analizom napona i deformacije pod jednoosnim opterećenjem. Rezultati su pokazali da hibridno armiranje vlaknima značajno poboljšava čvrstoću na pritisak (do ~45 MPa), zateznu čvrstoću i duktilnost nakon vršne pružne snage u poređenju sa običnim RAC-om. Digitalna obrada slike otkrila je prelaz sa lokalizovanih pukotina u kontrolnim i RAC mešavinama na distribuirane mikropukotine u hibridnim sistemima vlakana, što ukazuje na poboljšanu kontrolu pukotina i preraspodelu napona. Mikrostrukturna analiza korišćenjem skenirajuće elektronske mikroskopije (SEM) potvrdila je poboljšanje ITZ-a i efikasnu interakciju vlakana i matrice, gde su polipropilenska vlakna kontrolisala nastanak mikropukotina, a čelična vlakna premošćivala makropukotine. Performanse trajnosti procenjene su kroz apsorpciju vode i napad kiseline. Dok su reciklirani agregati povećali propustljivost, hibridni sistemi vlakana poboljšali su otpornost na širenje pukotina i održali strukturni integritet u agresivnim uslovima. Međutim, prekomerni sadržaj vlakana doveo je do povećane poroznosti, ističući potrebu za optimalnim doziranjem vlakana. Generalno, studija pokazuje da sinergistička interakcija između čeličnih i polipropilenskih vlakana može efikasno ublažiti nedostatke RAC-a i proizvesti izdržljiv, duktilan i visokoperformansni održivi beton pogodan za strukturne primene.

Ključne reči: *Reciklirani agregat, čelična vlakna, polipropilenska vlakna, hibridna vlakna. digitalna obrada slike, mikrostrukturna analiza, Studija trajnosti.*

Naučni rad
Rad primljen: 11.01.2026.
Rad korigovan: 08.04.2026.
Rad prihvaćen: 23.04.2026.